Supporting Information

Mesoporous cobalt-iron-organic frameworks: plasma-enhanced oxygen evolution electrocatalyst

Wenxia Chen[a], Yiwei Zhang[a*], Guangliang Chen[b], Rong Huang[a], Yuming Zhou[a*], Yangjin Wu[a], Yinjie Hu [c*], Kostya (Ken) Ostrikov[d]

[a]School of Chemistry and Chemical Engineering, Southeast University, Jiangsu Optoelectronic Functional Materials and Engineering Laboratory, Nanjing 211189, P. R. China.

[b]Key Laboratory of Advanced Textile Materials and Manufacturing Technology and Engineering Research Center for Eco-Dyeing & Finishing of Textiles, Ministry of Education, Zhejiang Sci-Tech University, Hangzhou 310018, P. R. China.

[c]Key Laboratory of Advanced Functional Materials of Nanjing, Nanjing Xiaozhuang University, Nanjing 211171, China.

[d]School of Chemistry, Physics and Mechanical Engineering, Queensland University of Technology, Brisbane, QLD 4000, Australia.

[*]Corresponding authors. E-mail: zhangchem@seu.edu.cn, ymzhou@seu.edu.cn, huyj113@qq.com. Tel: +86 25 52090617; Fax: +86 25 52090617.

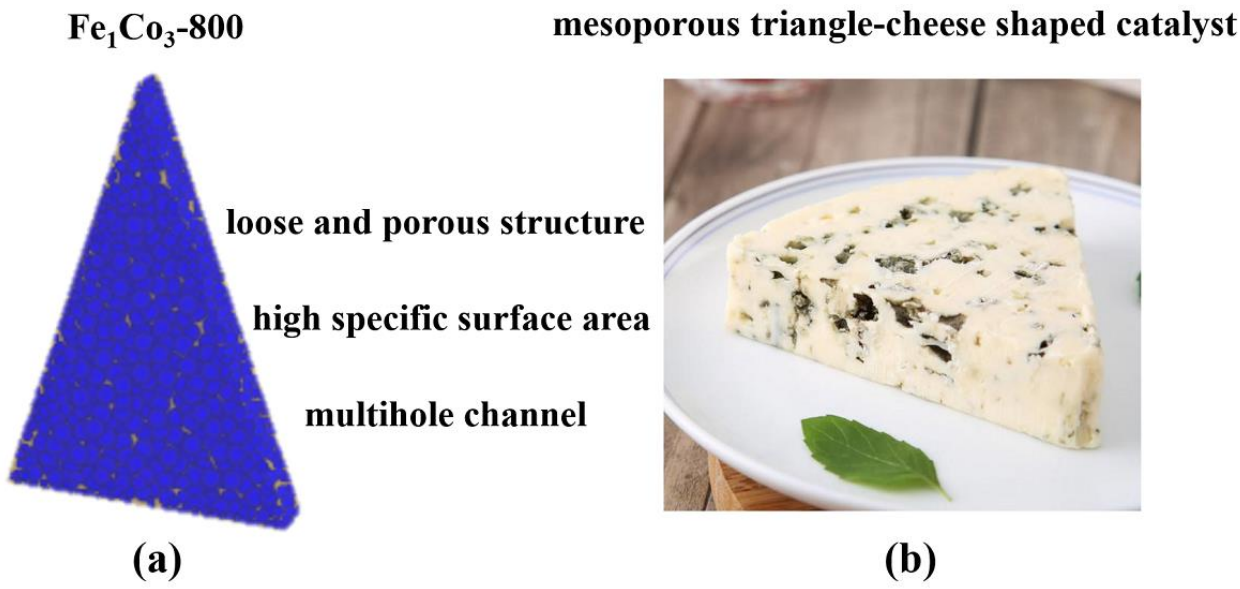

Scheme S1 Multichannel structure of (a) Fe_1Co_3-800, (b) mesoporous triangle-cheese shaped catalyst.

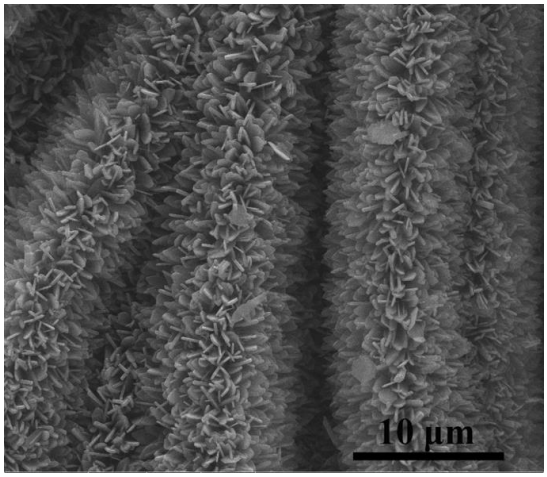

Fig. S1 SEM images of original Co-MOF@CC.

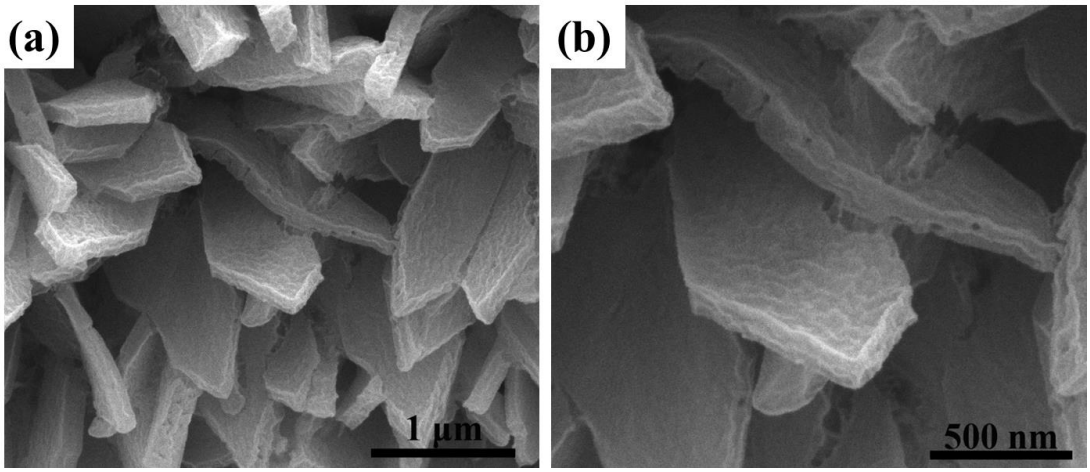

Fig. S2 (a) and (b) SEM images of Co-MOF@CC modified by O_2-Ar plasma at 100 W.

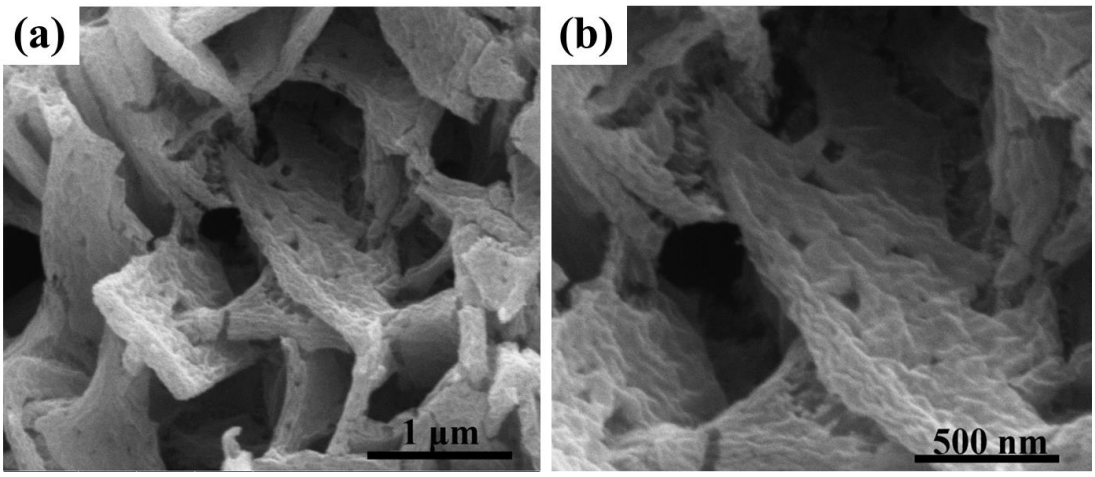

Fig. S3 (a) and (b) SEM images of Co-MOF@CC modified by O_2-Ar plasma at 150 W.

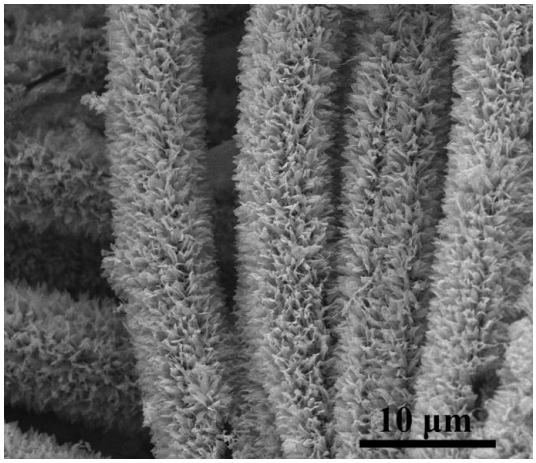

Fig. S4 SEM images of Co-MOF@CC modified by O_2-Ar plasma at 180 W.

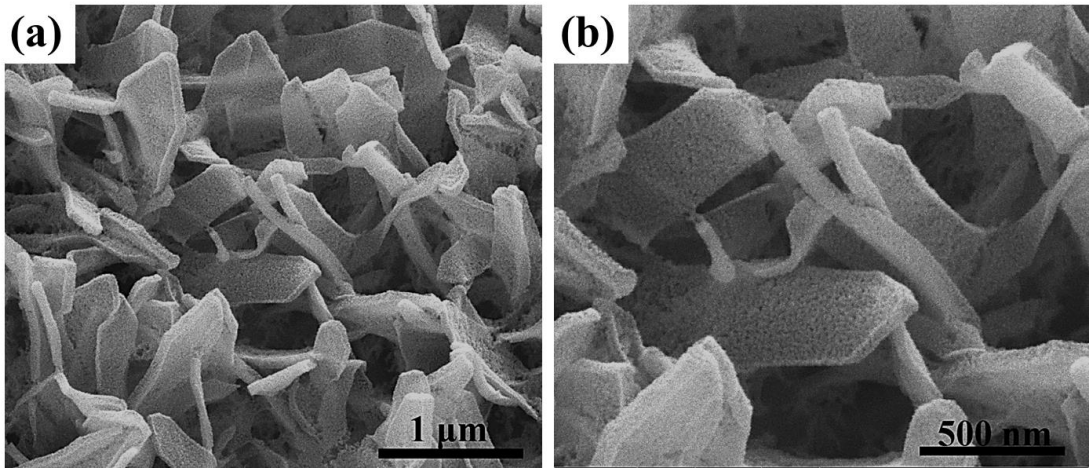

Fig. S5 (a) and (b) SEM images of Co-MOF@CC modified by O_2-Ar plasma at 200 W.

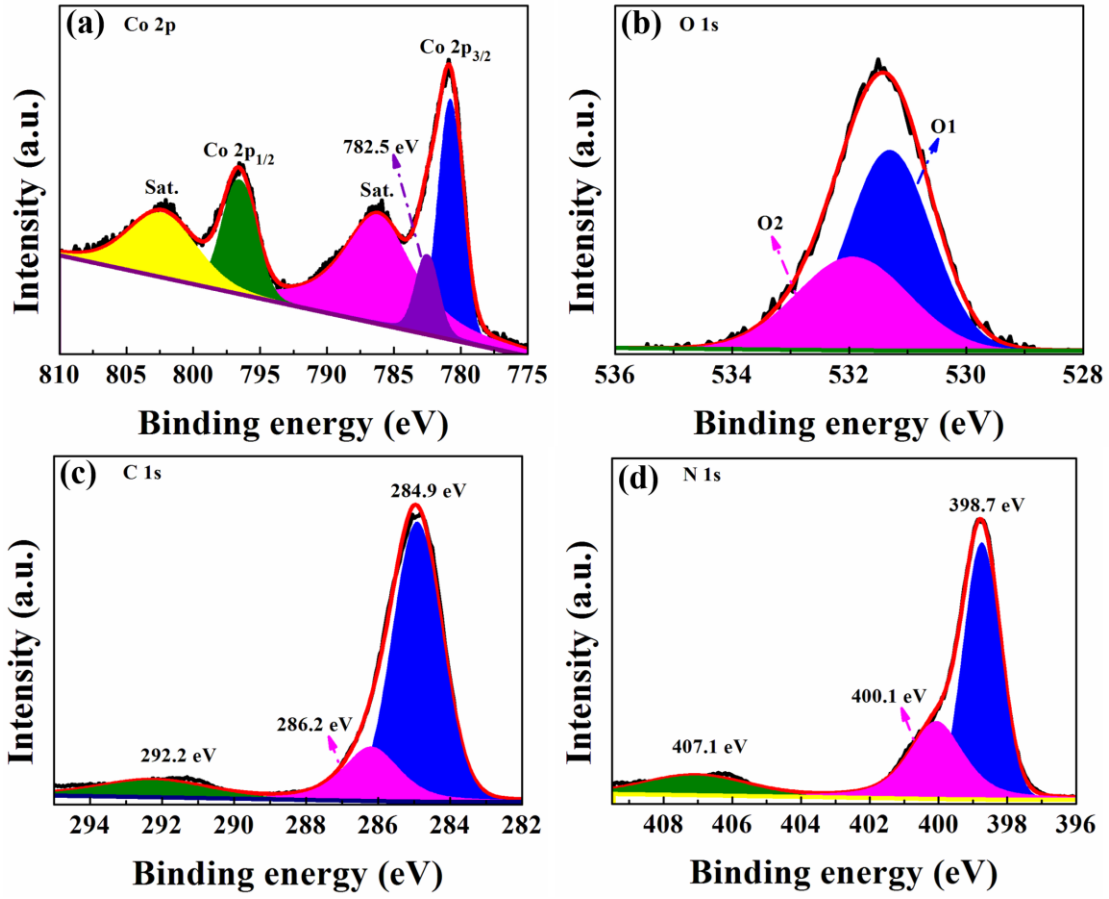

Fig. S6 XPS spectra of (a) Co 2p, (b) O 1s, (c) C 1s and (d) N 1s regions for the 2D Co-MOF samples.

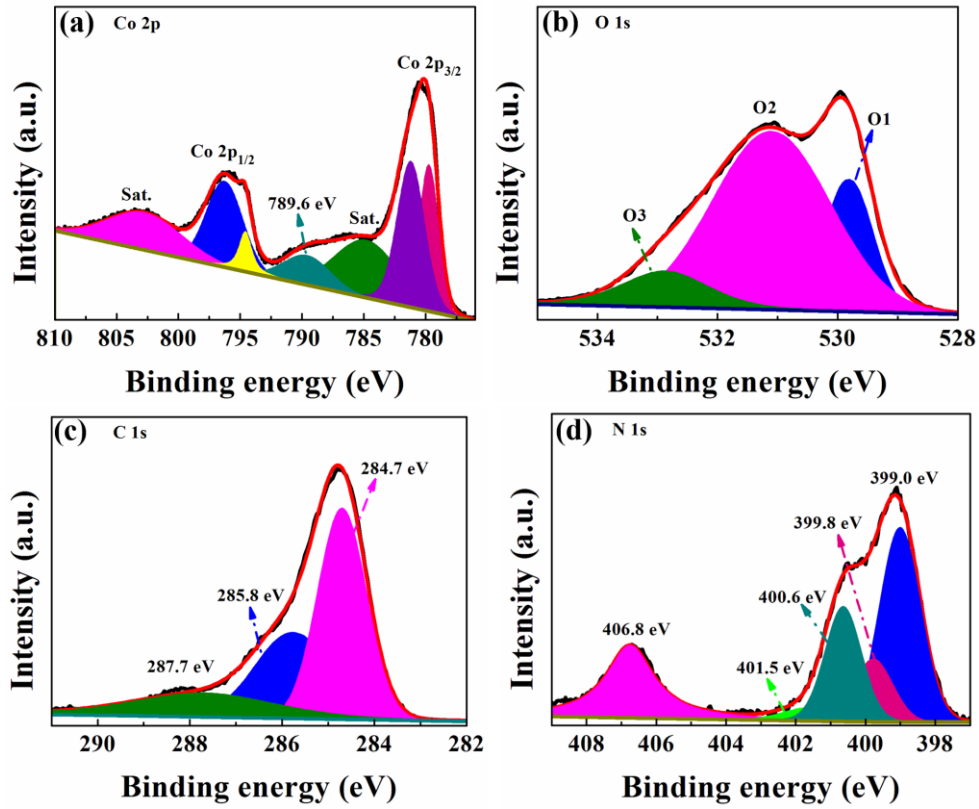

Fig. S7 XPS spectra of (a) Co 2p, (b) O 1s, (c) C 1s and (d) N 1s regions for the 2D Co-MOF samples treated by O_2-Ar RF plasma with 180 W power.

For C 1s spectrum, it can be curved into three peak components located at 284.7, 285.8 and 287.7 eV, which are assigned to C-C, C-N and C=O, respectively. Compared to the 2D Co-MOF samples, the negative shift of binding energy is about 4.5 eV for C 1s at 287.7 eV, suggesting the transition of $\pi \rightarrow \pi^*$ to C=O groups. It confirms that the elemental chemical component of the 2D Co-MOF samples have changed by O_2-Ar RT plasma effect. The N 1s at 398.7, 400.1 and 407.1 eV are relevant to pyridine-like N, pyrrole-type N and oxidized N varieties in original 2D Co-MOF, respectively (Fig. S 6d). Nevertheless, the increased graphitic-N at 400.6 and 401.5 eV can enhance conductivity of the material and promote electronic transfer rapidly (Fig. S 7d).

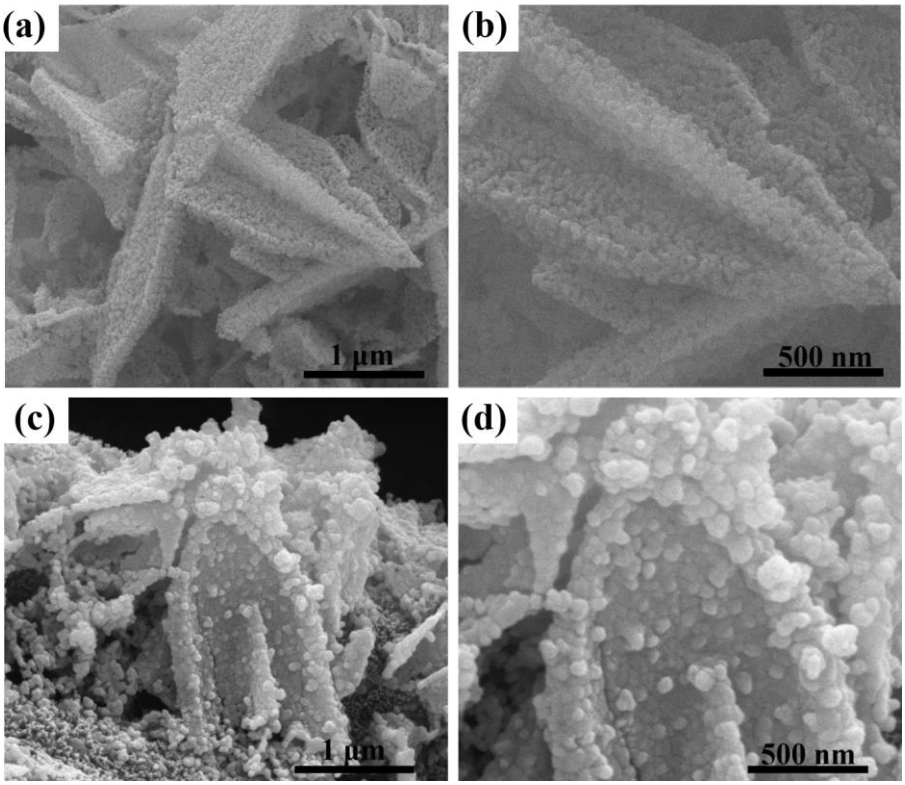

Fig. S8 SEM images of (a) and (b) Fe_1Co_3/V_O-700, (c) and (d) Fe_1Co_3/V_O-900 with O_2-Ar RF plasma treatment.

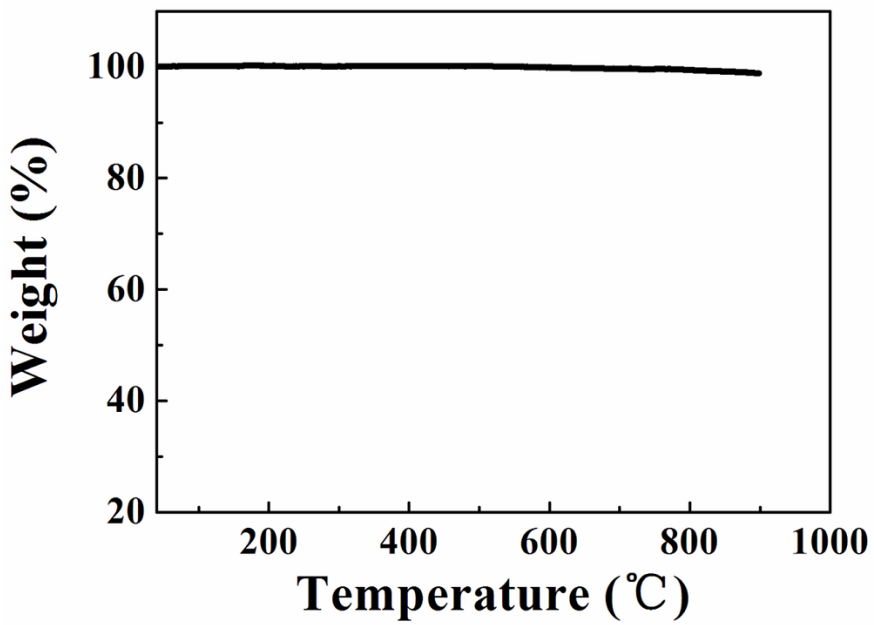

Fig. S9 Thermogravimetric analysis (TGA) curve of the Fe_1Co_3/V_O-800 under N_2 with a ramp of 10 °C · min^{-1}.

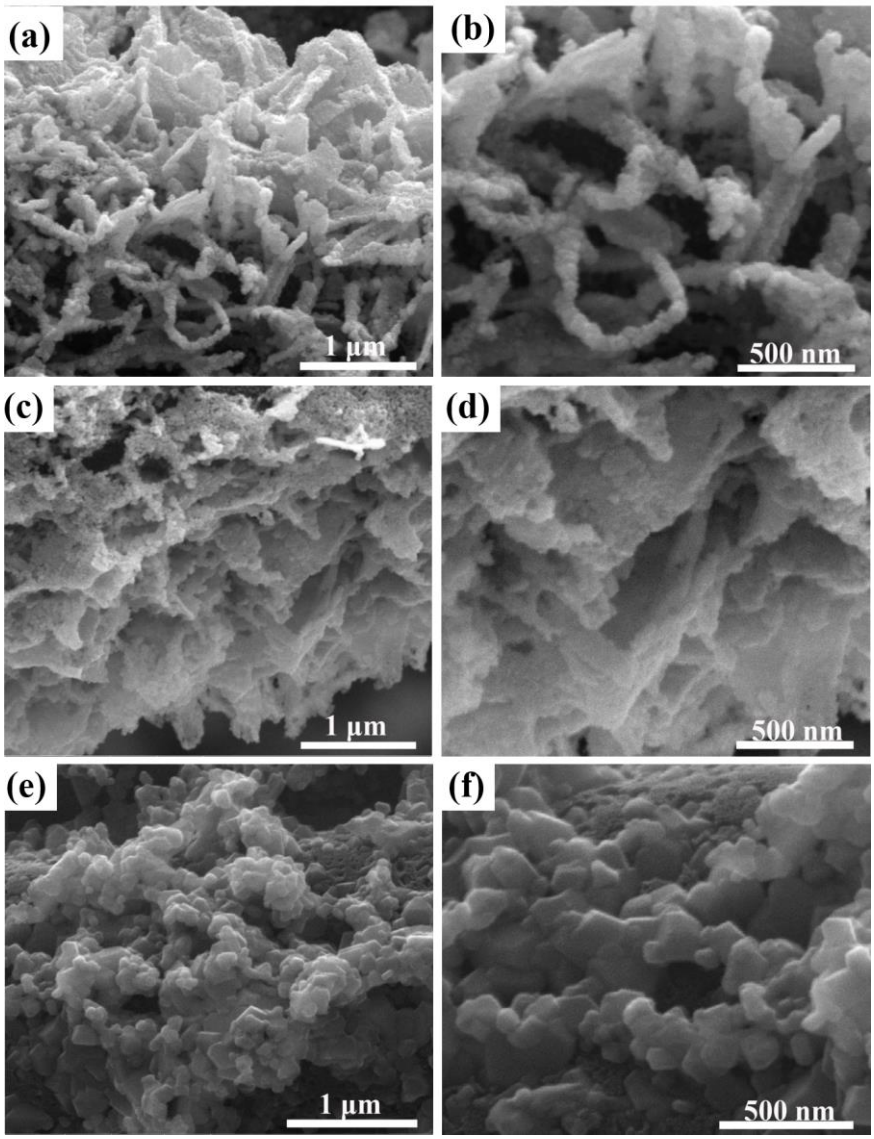

Fig. S10 SEM images of (a) and (b) Fe_1Co_3-700, (c) and (d) Fe_1Co_3-800, (e) and (f) Fe_1Co_3-900 without using O_2-Ar RF plasma treatment.

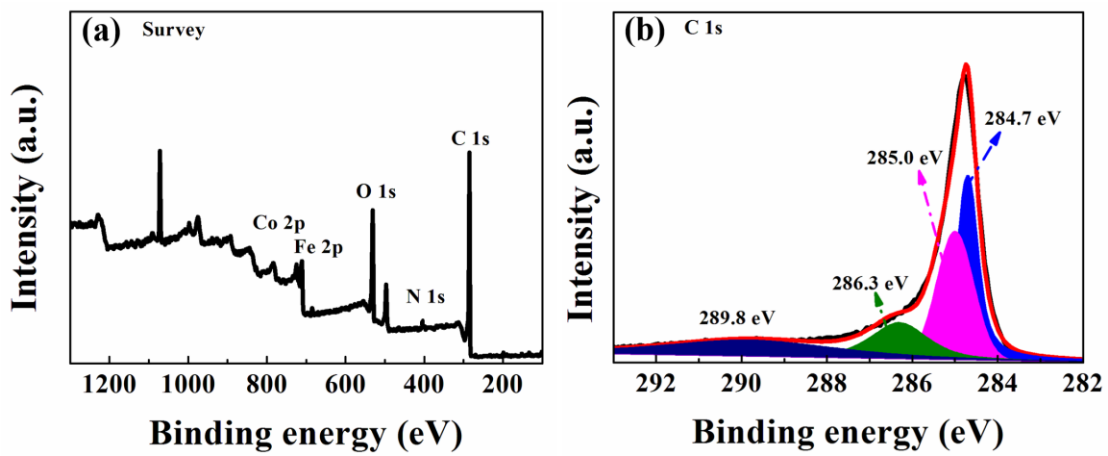

Fig. S11 XPS spectra of (a) survey and (b) C 1s of the Fe_1Co_3/V_O-800 samples treated by O_2-Ar RF plasma with 180 W power.

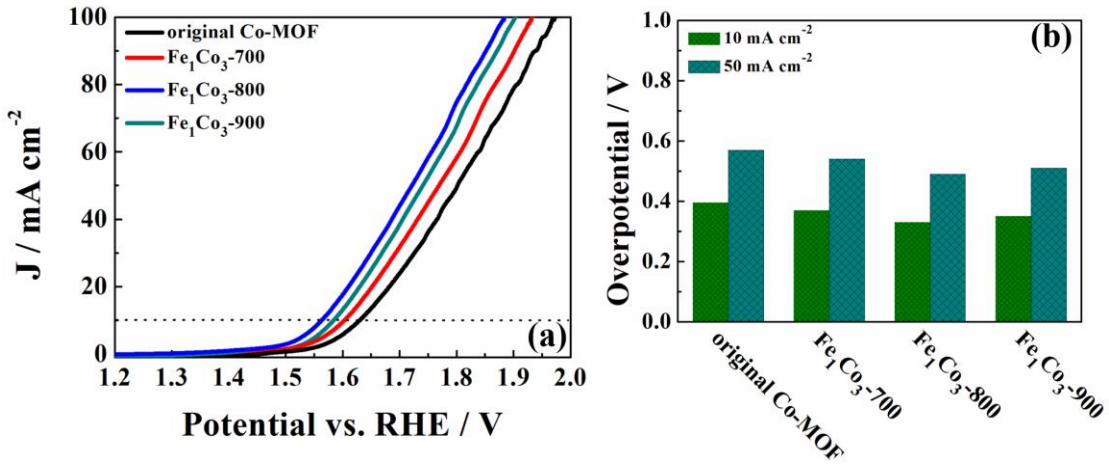

Fig. S12 (a) LSV polarization curves of original Co-MOF, Fe_1Co_3-700, Fe_1Co_3-800 and Fe_1Co_3-900 without using O_2-Ar RF plasma treatment at the scan of 5 mV s^{-1}, and (b) the corresponding overpotential.

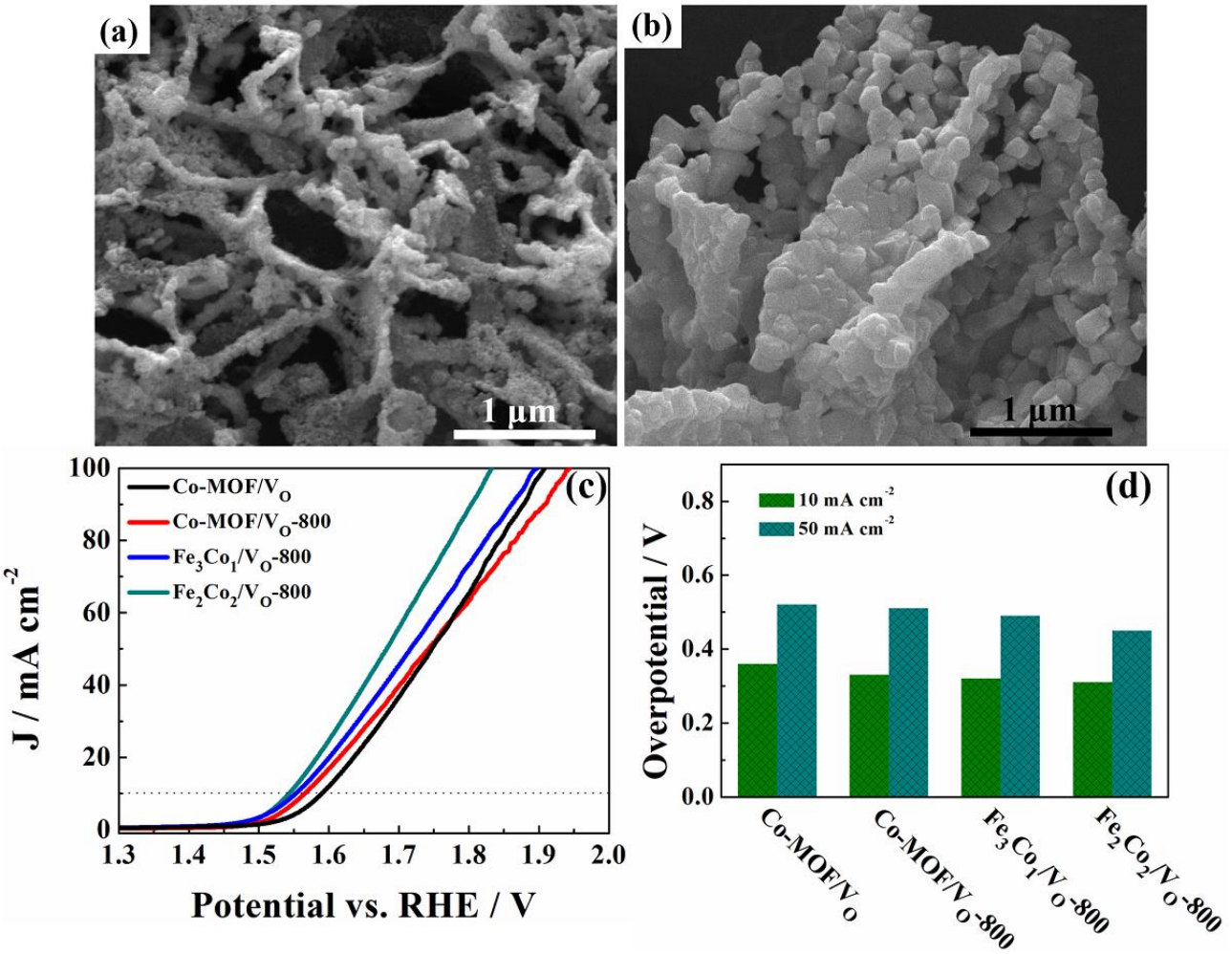

Fig. S13 SEM images of (a) Fe_2Co_2/V_O-800 and (b) Fe_3Co_1/V_O-800, (c) LSV polarization curves of Co-MOF, Co-MOF/V_O-800, Fe_2Co_2/V_O-800 and Fe_3Co_1/V_O-800 modified by O_2-Ar RF plasma, and (d) the corresponding overpotential.

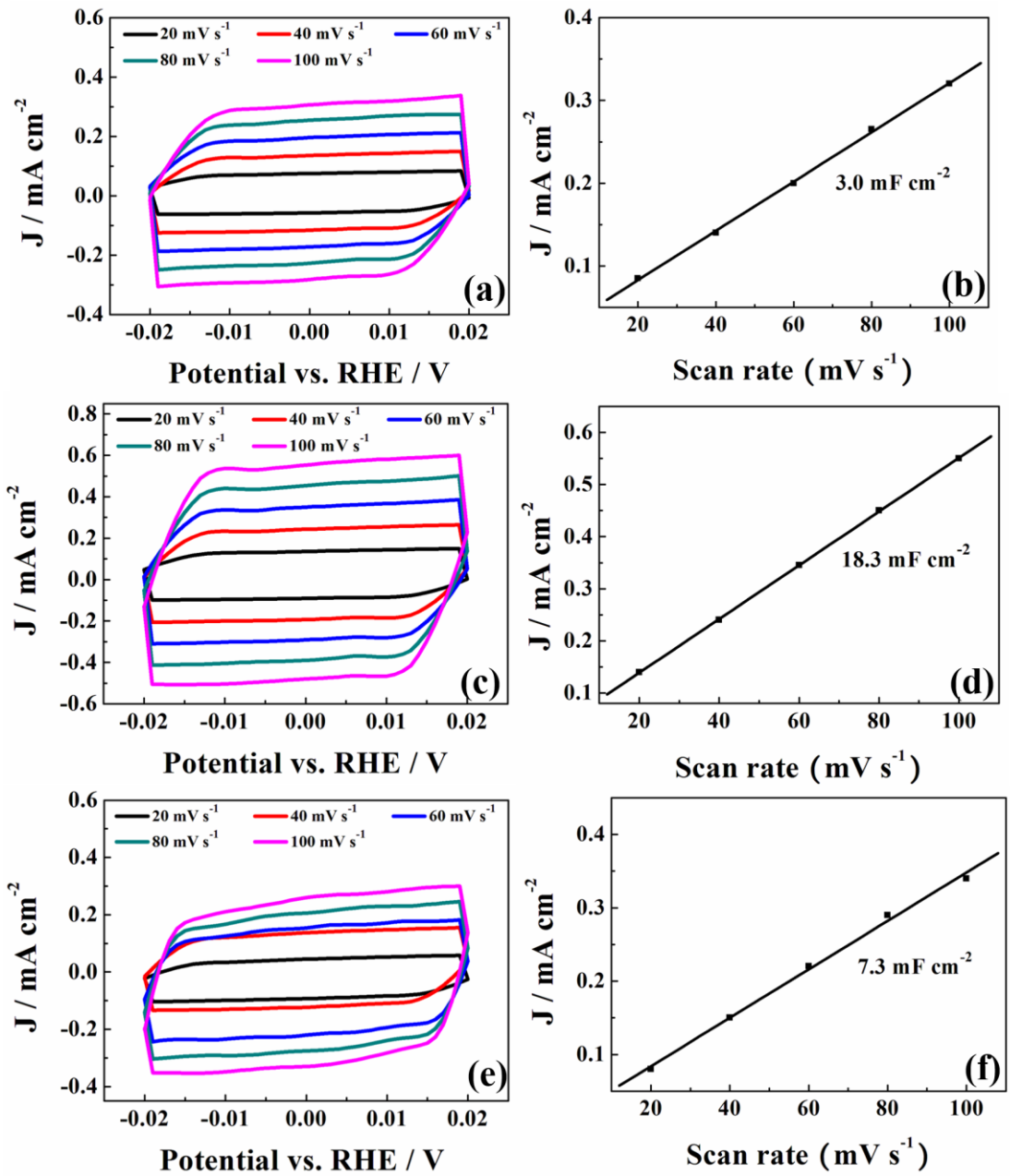

Fig. S14 CV curves in a potential range of -0.02-0.02 V versus RHE of (a) Fe_1Co_3/V_O-700, (c) Fe_1Co_3/V_O-800, (e) Fe_1Co_3/V_O-900, and (b), (d) and (f) the corresponding current density difference at 0 V plotted against scan rate in a non-Faradaic range.

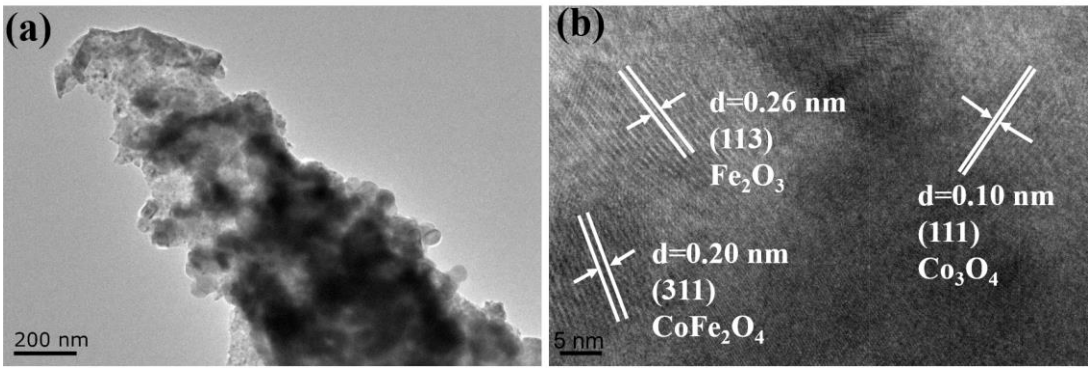

Fig. S15 (a) TEM and (b) HRTEM images of Fe_1Co_3/V_O-800 after OER testing.

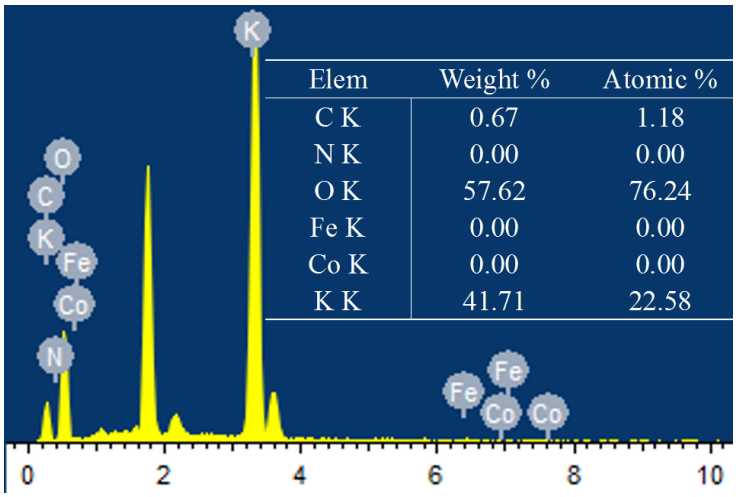

Elem	Weight %	Atomic %
C K	0.67	1.18
N K	0.00	0.00
O K	57.62	76.24
Fe K	0.00	0.00
Co K	0.00	0.00
K K	41.71	22.58

Fig. S16 The EDX spectral analysis of the electrolytes after the OER of the Fe_1Co_3/V_O-800 catalyst.

Table S1 Summary of the atomic compositions of the Fe_1Co_3/V_O-800 before and after OER calculated with the XPS data.

Sample	Atomic concentration (%)					Atomic ratio
	C	N	O	Fe	Co	Co/Fe
Before OER	72.31	2.77	19.81	1.25	3.86	3.08
After OER	63.84	2.68	28.49	1.19	3.80	3.19

Table S2 The comparison of OER activities for various catalysts.

Materials	Supports	Electrolytes	$E_{J=10mAcm^{-2}}$(V)	References
Fe_1Co_3/V_O-800	Carbon cloth	1 M KOH	1.49	This work
Co-Pt/C	Carbon cloth	1 M KOH	1.55	1
Hollow Mo-CoOOH nanoarrays	Carbon cloth	1 M KOH	1.535	2
Co^{2+}-buserite	Carbon cloth	1 M KOH	1.607	3
CoO@FeOOH-NWAs	Carbon cloth	1 M KOH	1.71	4
CoP	Carbon cloth	1 M KOH	1.511	5
Fe-CoP	Carbon cloth	1 M KOH	1.612	6
PANI-FeCo/MWCNT	Carbon cloth	1 M KOH	1.51	7
meso/micro-FeCo-N_x-CN-30	Carbon cloth	1 M KOH	1.60	8

References

1 Hong Zhang, Yanyu Liu, Haijun Wu, Wei Zhou, Zongkui Kou, Stephen John Pennycook , Jianping Xie, Cao Guan and John Wang, J. Mater. Chem. A, 2018, **6**, 20214-20223.

2 C. Guan, W. Xiao, H. J. Wu, X. M. Liu, W. J. Zang, H. Zhang, J. Ding, Y. P. Feng, S. J. Pennycook, J. Wang, Nano Energy, 2018, **48**,73-80.

3 M. Nakayama, K. Fujimoto, T. Kobayakawa and T. Okada, Electrochem. Commun., 2017, **84**, 24-27.

4 Y. Wang, Y. M. Ni, B. Liu, S. X. Shang, S. Yang, M. H. Cao, C. W. Hu, Electrochim. Acta, 2017, **257**, 356-363.

5 P. Wang, F. Song, R. Amal,Y. H. Ng, X. L. Hu, ChemSusChem, 2016, **9**, 472-477.

6 M. Ma, G. L. Zhu, F. Y. Xie, F. L. Qu, Z. A. Liu, G. Du, A. M. Asiri, Y. D. Yao, X. P. Sun, ChemSusChem, 2017, **10**, 3188-3192.

7 C. C. Zhao, Y. H. Jin, X. Du, W. B. Du, J. Power Sources, 2018, **399**, 337-342.

8 S. Li, C. Cheng, X. J. Zhao, J. Schmidt, A. Thomas, Angew. Chem., Int. Edit., 2018, **57**, 1856-1862.